Atmos. Chem. Phys., 11, 6855–6870, 2011
www.atmos-chem-phys.net/11/6855/2011/
doi:10.5194/acp-11-6855-2011

Atmospheric Chemistry and Physics

The CO_2 release and Oxygen uptake from Fossil Fuel Emission Estimate (COFFEE) dataset: effects from varying oxidative ratios

J. Steinbach[1,*], C. Gerbig[1], C. Rödenbeck[1], U. Karstens[1], C. Minejima[2,], and H. Mukai[2]**

[1]Max Planck Institute for Biogeochemistry, Jena, Germany
[2]Center for Global Environmental Research, National Institute for Environmental Studies, Tsukuba, Japan
[*]now at: Stockholm University, Department of Applied Environmental Science, Stockholm, Sweden
[**]now at: Tokyo University of Agriculture and Technology, Department of Chemical Engineering, Tokyo, Japan

Received: 15 February 2011 – Published in Atmos. Chem. Phys. Discuss.: 21 February 2011
Revised: 25 May 2011 – Accepted: 6 July 2011 – Published: 18 July 2011

Abstract. We present a global dataset of CO_2 emissions and O_2 uptake associated with the combustion of different fossil fuel types. To derive spatial and temporal patterns of oxygen uptake, we combined high-resolution CO_2 emissions from the EDGAR (Emission Database for Global Atmospheric Research) inventory with country level information on oxidative ratios, based on fossil fuel consumption data from the UN energy statistics database. The results are hourly global maps with a spatial resolution of $1^\circ \times 1^\circ$ for the years 1996–2008. The potential influence of spatial patterns and temporal trends in the resulting O_2/CO_2 emission ratios on the atmospheric oxygen signal is examined for different stations in the global measurement network, using model simulations from the global TM3 and the regional REMO transport model. For the station Hateruma Island (Japan, 24°03′ N, 123°48′ E), the simulated results are also compared to observations. In addition, the possibility of signals caused by variations in fuel use to be mistaken for oceanic signals is investigated using a global APO inversion.

1 Introduction

High-precision measurements of atmospheric oxygen play an increasingly important role in our understanding of the global carbon cycle (see e.g. Keeling et al., 1993; Battle et al., 2000; Bender et al., 1998; Manning and Keeling, 2006) The close coupling between oxygen and carbon cycle results in anti-correlated changes in the atmospheric CO_2 and O_2 mixing ratios for almost all major exchange mechanisms: Photosynthesis in the terrestrial biosphere produces oxygen and consumes CO_2 whereas fossil fuel combustion consumes O_2 and produces CO_2. Only ocean-related changes are decoupled in the carbon-oxygen system, which allows the separation of oceanic and terrestrial carbon sinks through the use of atmospheric oxygen measurements (Keeling and Shertz, 1992). Additional information can be gained from the fact that the terrestrial processes can be distinguished by their oxidative ratios. The oxidative ratio of a process is defined as the number of O_2 moles that are consumed per mole CO_2 emitted in the process: $\mathrm{OR} = -\Delta O_2\,[\mathrm{mol}]/\Delta CO_2\,[\mathrm{mol}]$. For terrestrial photosynthesis and respiration, the average oxidative ratio is $\alpha_B = 1.1$ (Severinghaus, 1995), whereas it is $\alpha_F = 1.4$ for fossil fuel combustion and cement production (Keeling, 1988). These values represent global averages; the oxidative ratio can vary over spatial and temporal scales, depending on which elements other than carbon are involved in the specific oxidation process. In the case of fossil fuel burning, the oxidation process can be described as (Keeling, 1988):

$$\mathrm{CH_wO_xS_yN_z} + \left(1 + \frac{w}{4} - \frac{x}{2} + \frac{3}{2}y + \frac{5}{4}z\right)\mathrm{O_2} \quad (1)$$
$$\rightarrow \mathrm{CO_2} + \left(\frac{w}{2} - y - \frac{z}{2}\right)\mathrm{H_2O} + y\mathrm{H_2SO_4} + z\mathrm{HNO_3}$$

Here $\mathrm{CH_wO_xS_yN_z}$ represents the composition of the fuel. However, in most cases the sulfur and nitrogen content of fuels is negligible compared to the carbon and hydrogen content, therefore we adopt the following simplified formula:

$$\mathrm{C_xH_y} + \left(x + \frac{y}{4}\right)\mathrm{O_2} \rightarrow x\mathrm{CO_2} + \frac{y}{2}\mathrm{H_2O} \quad (2)$$

Hence the oxidative ratio OR_{ff} of the combustion can mainly vary between 1 to 2, with the ratio being 1 for pure

Correspondence to: J. Steinbach
(julia.steinbach@itm.su.se)

carbon and 2 for methane. Usually, the following oxidative ratios are used for the three main types of fossil fuel: 1.17 for coal (or solid fuels in general), 1.44 for oil and other liquid fuels, and 1.95 for gaseous fuels (Keeling, 1988). Cement production, accounting for 7 % of total anthropogenic CO_2 emissions, does not consume oxygen and thus has an oxidative ratio of 0.

For the partitioning of global carbon sinks as well as for interpretation of atmospheric O_2 and CO_2 signals measured at monitoring stations, usually the global average value $\alpha_F = 1.4$ is used. However, in some cases deviations from this average caused by the local fuel mix have already been observed: In the Netherlands, a region with high usage of natural gas, oxidative ratios as high as 1.5 have been measured (van der Laan-Luijkx et al., 2010; Sirignano et al., 2010). At the Japanese island Hateruma, observed pollution events (Minejima et al., 2011) have shown oxidative ratios ranging from 0.96 to 1.71, correlated with the origin of the air – either being from China (OR_{ff}∼1.11), Korea (OR_{ff}∼1.31) or Japan (OR_{ff}∼1.37). (The OR_{ff} given in brackets are national averages, which we have calculated using the fuel mix of the respective country. For this purpose, we have used national CO_2 emissions caused by the combustion of coal, oil and gas from Carbon Dioxide Information Analysis Center (CDIAC) inventory (Boden et al., 2009)).

To investigate whether – and where – information on the local fuel mix can be helpful for interpreting atmospheric CO_2 and O_2 signals, we have created time-dependent high-resolution global maps of the oxygen uptake associated with fossil fuel burning that can be used as input for global and regional models. These maps show where significant deviations from the global average α_F exist and need to be taken into account. In the following, Section 2 describes the methodology of creating the dataset for these uptake maps; Section 3 shows spatial patterns and temporal trends in the resulting O_2/CO_2 ratios, including the influence of their variation on the calculation of global land and ocean carbon budgets. In Sect. 4, the potential influence of the variations in fossil fuel mix on the atmospheric oxygen signal is investigated for different stations in the global measurement network, using a global and regional atmospheric transport model. The simulated results are compared to observations from a selected station, Hateruma Island. In Sect. 5, we investigate the possibility of mistaking variations in fossil fuel use for ocean signals when calculating APO fluxes with inverse methods. Section 6 concludes the paper.

2 The COFFEE dataset: data and methodology

To estimate spatial and temporal patterns in O_2/CO_2 emission ratios, high-resolution CO_2 emissions were combined with oxidative ratios at the national level derived from fuel consumption statistics, as illustrated in Fig. 1. High-resolution CO_2 emissions ((1) in Fig. 1) are taken from

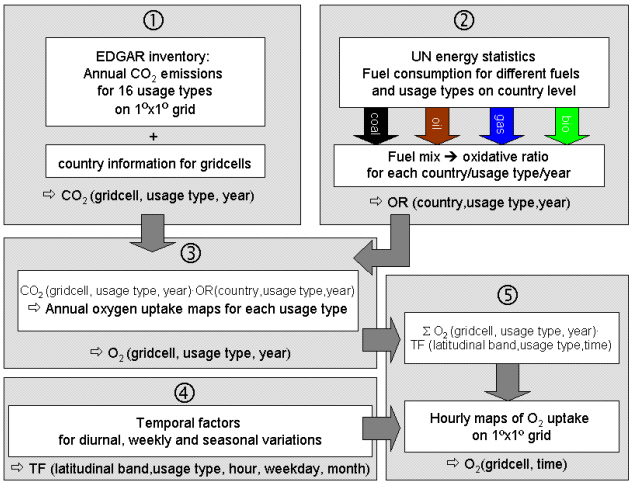

Fig. 1. Information flow for creation of the COFFEE dataset, using high resolution CO_2 emissions (EDGAR) and fuel-type specific fuel consumption (UN). See Sect. 2 for detailed explanation.

the *Emission Database for Global Atmospheric Research* (EDGAR, Olivier and Berdowski, 2001). We use EDGAR version 3.2, containing annual CO_2 emissions on a $1° \times 1°$ grid, that are split into 16 usage types (e.g. power generation, transport). The original emissions were available until the year 1995, an extension 1996–2001 was provided by S. Houweling (personal communication, 2004). This extension was performed consistently with the EDGAR methodology and used process-specific scaling factors given by J. Olivier. To allow comparison with recent atmospheric observations, the dataset was further extended until the year 2008 by keeping the spatial distribution and relative contributions of the different usage types from the year 2001 and extrapolating the amount of emissions using fuel consumption and cement production data at the national level (coal, oil and gas consumption data assembled by British Petroleum (BP, 2009), biofuel consumption from the United Nations (UN) Energy statistics (UN, 2009) and cement production data from the Carbon Dioxide Information Analysis Center (CDIAC, Boden et al., 2009)).

While the EDGAR data break down fossil fuel consumption by usage type, oxidative ratios are determined by the fuel type mix. Therefore, we use the energy statistics compiled by the United Nations Statistics Division (UN, 2009) to connect the usage types with their respective fuel mix (see Fig. 1, (2)) The UN dataset, currently available for the years 1991-2007, contains data on fuel production, import, export, consumption and conversion for 44 fuel types and over 200 countries. Fuel types include different sorts of coal, liquid and gaseous fuels as well as biofuels (e.g. fuelwood, biodiesel and various waste types). This dataset was chosen because the information on fuel consumption and conversion is not only given as national totals, but also split into different usage types. As in most cases the UN dataset has a more

detailed separation of usage types than EDGAR, the UN usage types were aggregated to match those from EDGAR. A list of all EDGAR usage types and the corresponding UN categories is given in Table 1 in the supplement to this paper. To calculate the fuel-mix-specific oxidative ratios from these consumption data, CO_2 emissions and oxygen uptake are at first derived for each fuel, country, usage type and year separately. CO_2 emissions are estimated from the carbon content of the consumed fuels, following the procedure and using the fuel-specific conversion factors from the 2007 statistics report by the International Energy Agency (IEA, 2007): Fuel consumption is first converted to a common energy unit (Terajoules) and then multiplied with carbon emission factors (CEF, given in tons of carbon per Terajoule). Full combustion of fuels is assumed. Therefore the resulting carbon emissions are not corrected for unoxidized carbon, which is also consistent with the EDGAR methodology. Instead of applying a general correction (in terms of a percentage) for carbon stored in non-energy products, only the usage types that actually produce CO_2 emissions were chosen.

For calculating the corresponding O_2 uptake, CO_2 emissions for each entry in the dataset were multiplied with their specific oxidative ratio. Different oxidative ratios were used for the four main fuel types: coal, oil, gas and biofuels. Note that variations within these fuel groups are rather small compared to the differences between the different fuel types, e.g. the ratio for different types of coal ranges from 1.09 to 1.18 (Keeling, 1988). For coal, oil and gas the aformentioned oxidative ratios are used. For biofuels a weighted average of 1.07 was taken. This value was determined by applying Eq. (1) to each of the biofuels present in the dataset and weighting their contributions by amount used.

CO_2 emissions and O_2 uptake for the different fuel types were added up for each country, usage type and year. The total O_2 uptake divided by the total CO_2 emissions gives the specific oxidative ratio for this set. After the calculation of oxidative ratios, the dataset was checked for missing values. These were replaced by "best estimate" oxidative ratios: If only single years were missing, oxidative ratios were interpolated from the surrounding years, and where no information existed for the whole usage type in a certain country, either the mean value for this usage type (for usage types with a special oxidative ratio, e.g. gas flaring) or the country mean was used. Since the fuel consumption data for the early 1990s seemed not very reliable, with unrealistically large variations and many missing values, only data from 1996 onward was used.

To derive the O_2 uptake at the gridcell level, the EDGAR CO_2 emissions for each usage type and year were multiplied by the obtained oxidative ratios for the country to which the respective gridcell belongs ((3) in Fig. 1). For the allocation of gridcells to countries, information from Brenkert (1996) was used. In case a gridcell belongs to several countries, CO_2 emissions are split up according to the different countries' population in the gridcell. Temporal factors ((4) in Fig. 1) for seasonal, weekly and daily cycles for the different usage types were applied to the resulting annual values of CO_2 emission and O_2 uptake. These temporal factors are based on a set of time profiles for the Netherlands that are provided in the EDGAR database (see (EDGAR/PBL, 2010) for a detailed description). For the use in COFFEE, we have modified the factors to provide a better global representation: Seasonal cycles in fuel use were reversed for the Extratropical Southern Hemisphere ($-90°$ to $-20°$). In the Tropics ($-20°$ to $20°$), the seasonal variations were suppressed for some usage types ("power generation" (F20/B20 in EDGAR)) and 'fossil fuel use from residentials, commercials and other sector' (F40/B40 in EDGAR). Note that the resulting temporal structure needs to be interpreted with care, as variations in fuel use for the different usage types can be quite different locally (see Sect. 3.2) To avoid discontinuities in the final time series, the original step functions for the seasonal cycles were smoothed by applying an exponentially weighted running-mean and using an iterative correction of the results to ensure the conservation of the annual mean. Finally, the sum of emissions and uptake over all usage types was calculated for each gridcell ((5) in Fig. 1). The resulting dataset consists of hourly fluxes of CO_2 emissions and O_2 uptake for the years 1996 to 2008. In the following, it will be referred to as the "**C**O_2 release and **O**xygen uptake from **F**ossil **F**uel **E**missions **E**stimate" (COFFEE) dataset. It is available for download at ftp://ftp.bgc-jena.mpg.de/pub/outgoing/coffee.

3 Spatial and temporal variations in fossil-fuel-related oxidative ratios

3.1 Spatial distribution

Figure 2 shows the resulting global maps of CO_2 emissions (a), O_2 uptake (b) and oxidative ratios OR_{ff} (c) as determined from the COFFEE dataset. All maps are annual averages for the year 2006. It can be seen that the patterns in oxygen uptake mostly follow the patterns of the CO_2 emissions. As expected, high CO_2 emissions occur mainly in the US, Europe and some parts of Asia, while they are rather low in South America and Africa. The lines between the continents represent ship tracks. The oxidative ratio, determined as the ratio of O_2 uptake to CO_2 emissions, covers the whole range from 0 to 1.95, with a spatial standard deviation of 0.2. For better visibility, the range of OR_{ff} in Fig. 2c is limited from 1 to 2, thus omitting a few gridcells with $OR_{ff} = 0$ that are caused by dominant cement production. The colors in Fig. 2c are representative of the fuel types the respective oxidative ratio would correspond to: green for biofuels, black for coal, brown for oil and blue for gas. In the US and most of Europe, OR_{ff} is close to the global average, as oil is the main fuel source. This is also the case for emissions caused by international shipping. Lower OR_{ff} are found in Africa and Eastern Asia, as fuel combustion in Africa

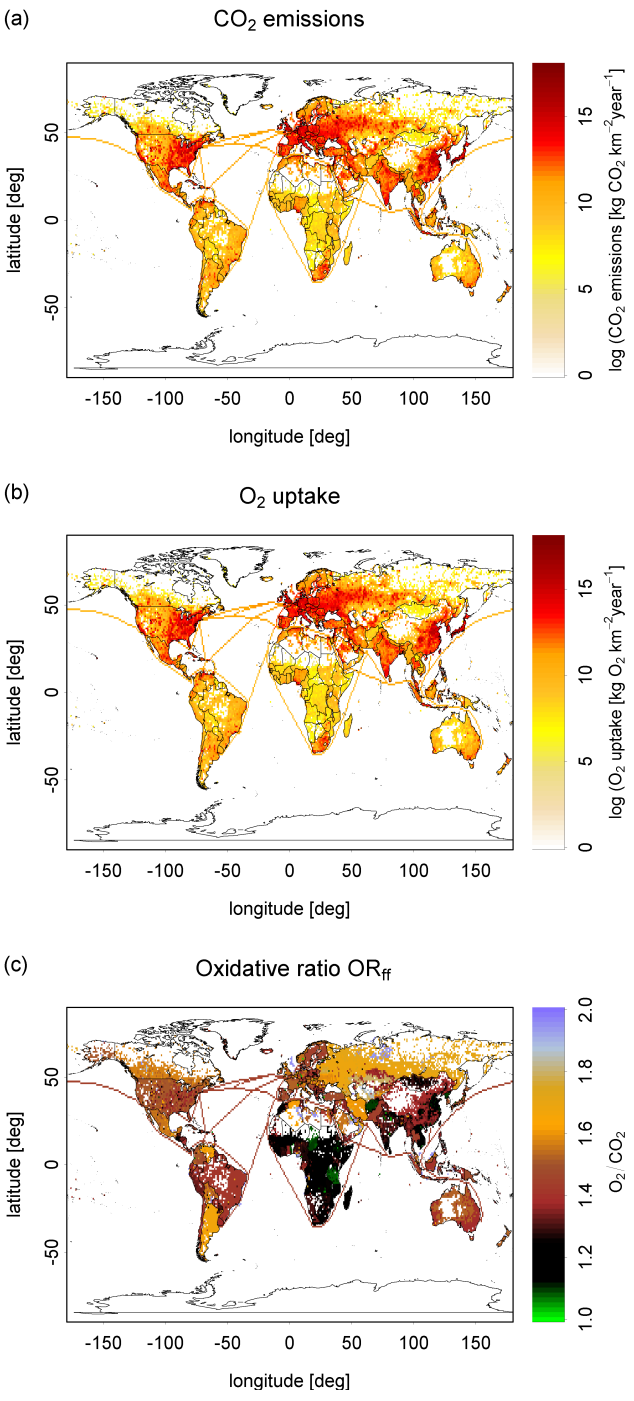

Fig. 2. Global maps of fossil-fuel-related CO_2 emissions **(a)**, oxygen uptake **(b)** and fossil-fuel-related oxidative ratios **(c)** for the year 2006 as calculated from the COFFEE dataset.

is dominated by a mix of biofuels (in this case traditional fuels as fuelwood and animal manure) and oil, whereas in Asian countries, like China and India, coal is the main fuel source. In China, cement production plays an important role as well, contributing to a further decrease in the ratio. A high contribution of gas can be seen in the oxidative ratios from e.g. Russia, Argentina and Canada. Blue and grey colors represent oxidative ratios above 1.8, where gas is the main source of fossil fuel burning, while the orange colors (representing ratios higher than 1.6) are a sign of significant contribution of gas to the fuel mix.

3.2 Temporal variations

In addition to these spatial variations, OR_{ff} can also vary temporally on different timescales, depending e.g. on seasonal and short-term variations in fuel use. The variations in CO_2 emissions and OR_{ff} on these timescales are shown in Fig. 3 (again for the year 2006, results for the other years are comparable).Variations are integrated over the three latitudinal bands Extratropical Northern Hemisphere (NH, +20° to +90°), Tropics (TR, −20° to +20°) and Extratropical Southern Hemisphere (SH, −90° to −20°). The upper row (Fig. 3a and b) shows the variation in CO_2 emissions, given in percent of the mean annual emission in the respective latitudinal band. For better visibility, different timescales are separated, with Fig. 3a showing the seasonal cycle (monthly averages), whereas short-term variations (hourly to weekly) are illustrated in Fig. 3b. The lower row (Fig. 3c and d) shows the respective plots for the variations in OR_{ff}. Note that these sub-annual variations reflect mainly the structure of the modified EDGAR time factors, on whose limitations one needs to be aware. Thus the purpose of this section is to show the resulting temporal structure in COFFEE as well as to point out some caveats for its interpretations.

Figure 3a shows that CO_2 emissions are always higher during each hemisphere's winter, as more fuel is used for heating purposes. (Heavy use of air conditioning in the summer is not taken into account in the EDGAR time profiles, but in reality this could cause a second peak in the summer in the warmer areas of the world.) With a range of about 30 % of the mean annual emissions, the seasonal cycle is more pronounced in the high latitudes than in the Tropics (18 %), as expected. Seasonal variations in the type of fuel used seem to be smaller than variations in the amount of fuel used, at least on these spatial scales: A clear seasonal cycle in OR_{ff}, however with an amplitude of merely 0.04, can only be seen for the Northern Hemisphere, whereas the time series for the SH and the Tropics are rather flat.

Figure 3b and d show hourly CO_2 emissions and OR_{ff} for one week in January, illustrating the additional short-term variations. For all latitudinal bands, CO_2 emissions exhibit a diurnal cycle: Emissions are higher during daytime than at night, and variations in transport lead to emission peaks in the morning and afternoon. Depending on the season, the relative contributions of the different usage types can change, so the diurnal cycle varies slightly in the course of the year, even though it always remains dominated by the double-peak structure of the transport emissions. One needs to consider that the use of a single set of temporal factors

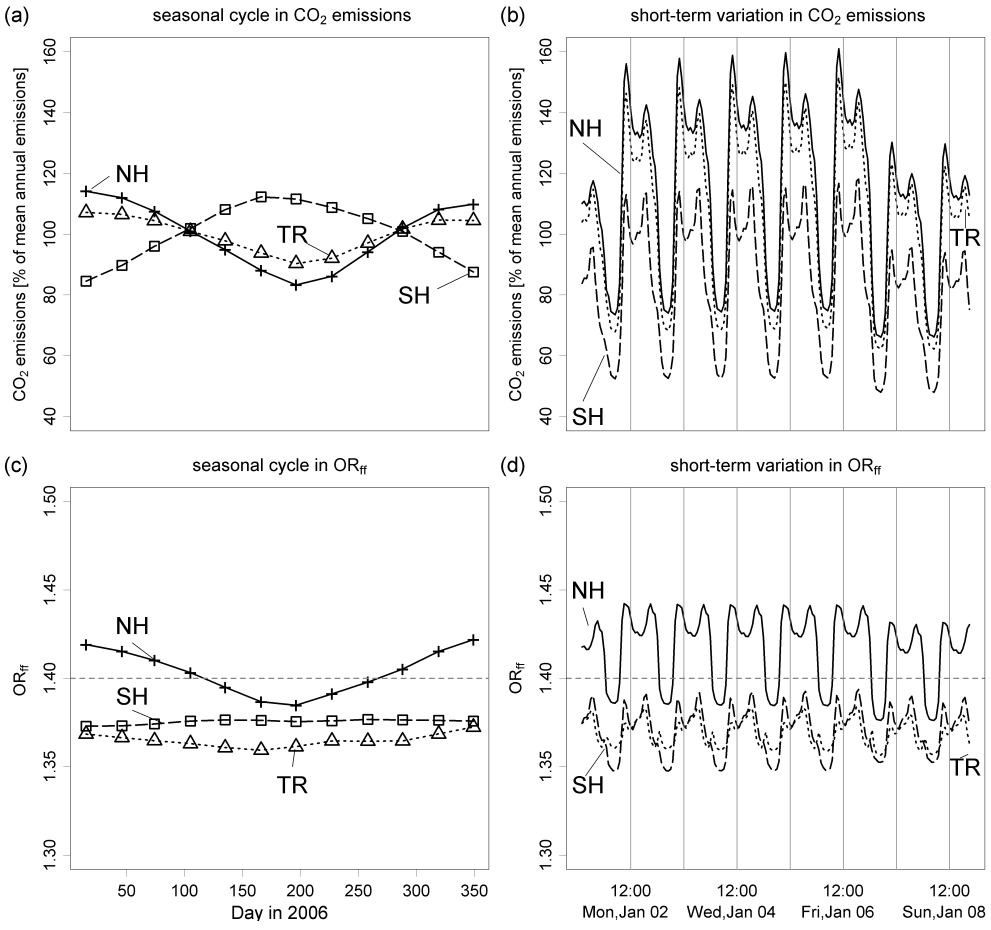

Fig. 3. Seasonal and short-term variations in CO_2 emissions (upper row, **a** and **b**) and OR_{ff} (lower row, **c** and **d**) for the year 2006, integrated over the three latitudinal bands NH, SH and Tropics (TR). The left column shows monthly averages for the whole year, illustrating the seasonal cycle; the right column short-term variations for the first week in January. Grey vertical lines in plots **(b)** and **(d)** indicate the local noon. CO_2 emissions are given in percent of the annual mean emissions in the respective latitudinal band. These annual mean emissions for NH, TR and SH correspond to a percentage of 89 %, 8 %, 3 % of the global emissions, respectively.

leads to an overestimation of the diurnal variation: In reality, the transport-related-peak does not occur everywhere at the same time, causing the peaks to smear out. The relative magnitude of the daily variations is slightly lower in the Southern Hemisphere (61 % peak-to-peak range) than in the Northern Hemisphere (83 %) and the Tropics (78 %). In addition, emissions are lower on the weekend, being about 85 % of the emissions during the week for all latitudinal bands (again, in reality, there is not such a clear separation, as the definition of "weekend" and the extent of fuel use on the working versus work-free days vary locally).

The oxidative ratio OR_{ff} also exhibits diurnal and weekly variations resembling the patterns in the CO_2 emissions. The fact that OR_{ff} is also highest in the morning and afternoon and lowest at night should not be misinterpreted as higher CO_2 emissions causing higher oxidative ratios. Instead variations in OR_{ff} are due to the temporal factors differing for the different usage types, thus the oxidative ratio is dominated by different usage types at different times of the day, e.g. by transport in the morning/afternoon. These differences in the temporal patterns are much smaller for the weekly cycle (all usage types either have lower emissions on the weekend or no weekly cycle at all). Therefore, the difference between weekdays and weekend is not as pronounced in OR_{ff} as it is in the CO_2 emissions. Altogether, the sub-annual temporal variations in OR_{ff} are thus small against the spatial variations, especially when taking into account that our time factors tend to overestimate the temporal variation.

Long-term trends in OR_{ff} over the COFFEE-period are shown in Fig. 4. Figure 4a shows the global trend on the gridcell level, determined from linear regressions for each pixel. Red colors indicate an increase and blue colors a decrease in OR_{ff}. There is no general positive or negative trend for this time period, rather tendencies in both directions for different regions. Maximal changes range from -0.2 to +0.3 per decade. Figure 4b shows a time series of the

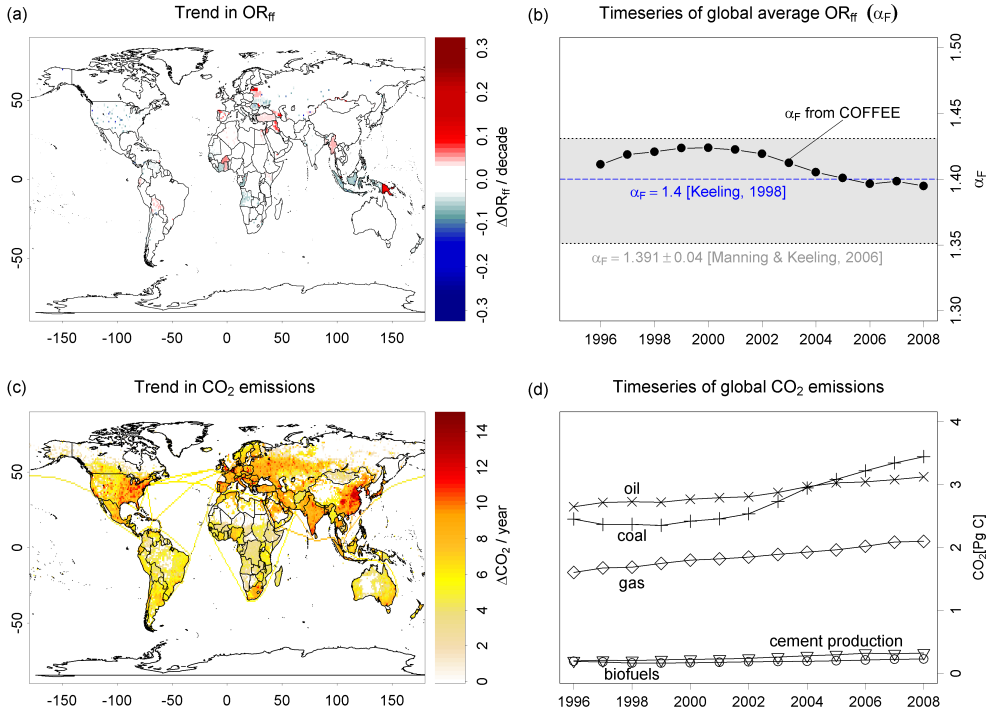

Fig. 4. Long-term changes in OR_{ff} and CO_2 emissions: **(a)** Trend in fossil-fuel-related oxidative ratio over the time period covered by the COFFEE dataset, calculated as the slope of a linear fit for each pixel. Red colors indicate an increase and blue colors a decrease in OR_{ff}. **(b)** Time series of global average oxidative ratio αF, derived from the COFFEE dataset. The blue line shows the value of 1.4 that is normally used for α_F, the grey rectangle shows the range of α_F for the 1990s as used by Manning and Keeling for their most recent calculation of global carbon sinks. **(c)** Trend in CO_2 emissions, calculated in analogy to the OR_{ff} trend in **(a)**. **(d)** Time series of global CO_2 emissions from different fuel types, as derived from COFFEE.

global average of OR_{ff} (in analogy to Sect. 1, the global average will be referred to as α_F in the following). The α_F obtained from the COFFEE dataset is close to the value of 1.4 that is normally used for fossil fuel burning (here shown as dashed blue line). Over the whole time period, α_F varies between 1.39 and 1.42, with a mean of 1.41 and a standard deviation of 0.01. Deviations from 1.4 are thus less than ±1.5 %. Again, no general trend is seen for the complete time series. However, starting from the year 2000, α_F is decreasing continuously. As seen in Fig. 4d, this trend can be explained by a strong increase in global CO_2 emissions from coal burning, including also a shift in the largest fuel emission source from oil to coal in the year 2005. Rather than by local changes in fuel use, this increase is caused by the strong growth of emissions from countries which rely primarily on coal, such as China. (Fig. 4c shows the global trend in CO_2 emissions trend on the gridcell level, derived from the COFFEE dataset in the same way as the trend in OR_{ff} for Fig. 4a). Note however that sudden rise of coal-related emissions after 2000 may be exaggerated, resulting from underestimated emissions before (Francey et al., 2010).

As a consistency check, we have compared the temporal variations and absolute values of α_F from COFFEE to the global averages derived from the BP (BP, 2009) and CDIAC (Boden et al., 2009) datasets. After correcting for the different fuel types included in the different datasets, the results do not significantly differ from our results.

The question now arises whether the variations in the global average are significant for the partitioning of global carbon sinks. The most recent sink estimate based on oxygen measurements has given a result of 1.9±0.6 and 1.2±0.8 Pg C/yr (for the period 1990–2006, with uncertainties given here as 1σ standard deviations) for the total oceanic and land biotic sink, respectively (Manning and Keeling, 2006). The uncertainty in α_F, assumed by Manning and Keeling as ±0.04, results in a significant contribution of ±0.2 Pg C/yr to the uncertainty of both sinks. However, Figure 4b shows that the temporal variations of α_F in COFFEE are about a factor 6 smaller than the uncertainty value of ±0.04 (here illustrated by the grey rectangle), thus resulting in maximum sink uncertainties of ±0.035 PgC/yr. This is consistent with Manning and Keeling's (2006) statement that temporal variations, in their case derived from CDIAC data for the 1990s, are not the major source of uncertainty in α_F. Their uncertainty is rather determined by the uncertainty in the absolute value, since interannual changes in fuel production or consumption are resolvable to a finer degree than the total production in any given year.

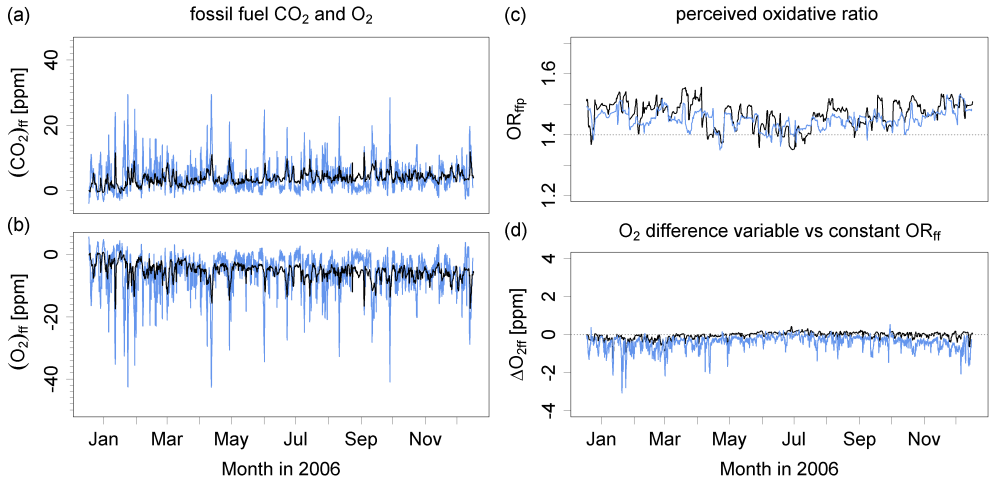

Fig. 5. Comparison of results from the global model TM3 (black) and the regional model REMO (blue) for the station Ochsenkopf (Germany). Fossil-fuel-related changes in the atmospheric mixing ratios of CO_2 **(a)** and O_2 **(b)** are shown on the left side. On the right side, **(c)** shows the perceived fossil-fuel-related oxidative ratio OR_{ffp}, and **(d)** the difference in the fossil-fuel-related O_2 signal calculated using the variable oxidative ratios from COFFEE instead of a constant oxidative ratio of 1.4.

4 Influence of fuel mix on atmospheric O_2 mixing ratio

4.1 Global and regional model simulations

The spatial and temporal variations in OR_{ff} shown above leave a signature in atmospheric oxygen that can potentially be seen in the network of oxygen measurements. For investigating this influence, CO_2 emissions and O_2 uptake from the COFFEE dataset were used as input for atmospheric transport models. Fossil-fuel-related changes in the atmospheric CO_2 and O_2 mixing ratios – hereafter called CO_{2ff} and O_{2ff} – were extracted from the simulations for a number of monitoring stations. Two different transport models were used: the global model TM3 (Heimann and Körner, 2003) and the regional model REMO (Langmann, 2000; Chevillard et al., 2002). TM3 provides worldwide coverage and therefore can give a complete overview of fossil-fuel-related effects. The advantage of REMO is its higher temporal and spatial resolution, which allows for better capturing of synoptic variations in fossil fuel use. REMO provides hourly output on a $0.5° \times 0.5°$ grid covering the area north of 30° N, whereas TM3 output is 6-hourly, and its finest resolution is $1.8° \times 1.8°$. Comparison of the CO_{2ff} and O_{2ff} results for stations that are within the domain of both models shows similar patterns in TM3 and REMO. An example is given in Fig. 5, containing simulations for the year 2006 at the station Ochsenkopf in Germany (50°01′49″ N, 11°48′39″ E, 1022 m a.s.l., see Thompson et al. (2009)). The simulated CO_{2ff} and O_{2ff} signals, shown in Fig. 5a and b, are dominated by synoptic scale pollution events rather than by seasonal or other periodic variations. As expected, the signals from the regional model show higher variability, resulting in sharper and taller peaks with increases in CO_2 and decreases in O_2. Figure 5c presents the perceived atmospheric oxidative ratio OR_{ffp} at the station location, derived from a running regression of O_{2ff} versus CO_{2ff}. As this perceived oxidative ratio is subject to atmospheric transport and mixing, it is not the same as the O_2/CO_2 ratio from the uptake/emissions of the respective gridcell. To get a signal representative for the synoptic time scale that dominates the atmospheric fossil fuel signal, a timeframe of 5 days was chosen for the regression. The negative slope of the O_{2ff} versus CO_{2ff} regression for a given 5-day-period corresponds to the perceived oxidative ratio OR_{ffp} at the middle of the time interval. The OR_{ffp} resulting from the two models do not show significant systematic differences. Both are varying between 1.35 and 1.56, with an average value slightly higher than α_F. In Figure 5d the difference $\Delta O_{2ff} = O_{2ff}\ (OR_{ff\mathrm{COFFEE}}) - O_{2ff}\ (OR_{ff} = 1.4)$ is shown, i.e. the difference between the fossil-fuel-related O_2 signal calculated using the variable oxidative ratios from COFFEE and the O_2 signal calculated a constant oxidative ratio of 1.4. As ΔO_{2ff} depends both on the size of fossil fuel signals and the deviation of the local fuel mix from the global average, it is significantly higher in the simulations from the regional model. In the example here, differences up to −3 ppm in the fossil-fuel-related O_2 signal are caused. Taking into account the typical measurement precision of 1ppm for atmospheric oxygen measurements, this deviation is quite small, but probably still detectable.

4.2 Comparison with observations from Hateruma Island

When interpreting fossil-fuel-related oxidative ratios, as shown in Fig. 5c, one needs to keep in mind that the total

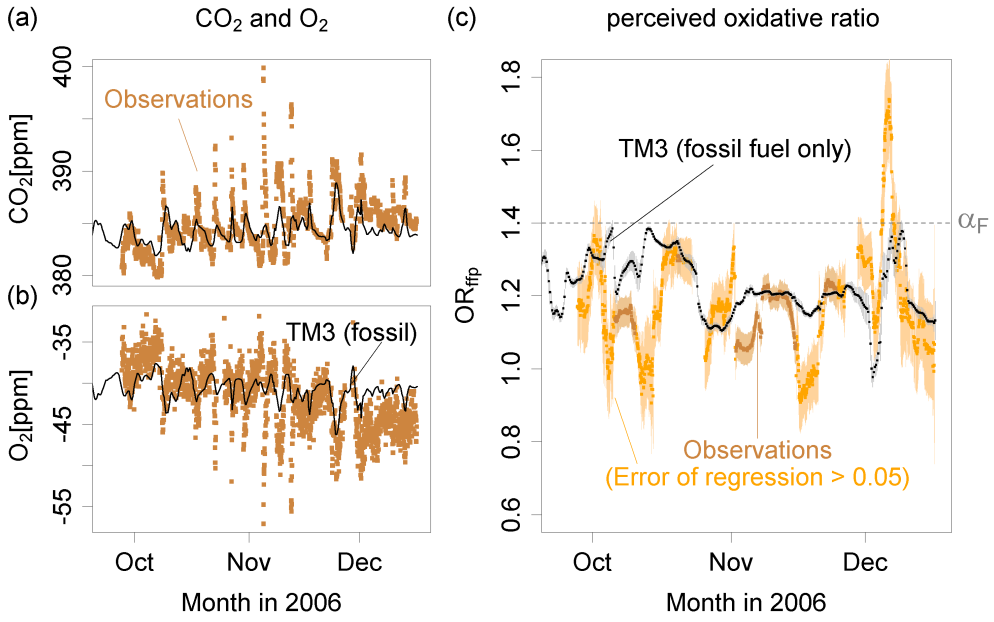

Fig. 6. Left: CO_2 **(a)** and O_2 **(b)** observations from Hateruma Island (brown dots), compared to CO_{2ff} and O_{2ff} simulations from the TM3 model (black lines). Right **(c)**: Oxidative ratios (corresponding color scheme) derived from linear regression of observed and simulated O_2 vs. CO_2. Shaded error bars show errors of the linear regression. Regressions with an error > 0.05 are considered as not sufficiently correlated and marked in orange.

oxidative ratio observable at a monitoring station is not only determined by fossil-fuel-related signals, but also by contributions from biospheric and oceanic processes. Whether a specific fuel signature can be seen in measured oxidative ratios at a given station depends on the size of fossil fuel signals compared to the atmospheric signals caused by other processes. This section examines oxidative ratios derived from CO_2 and O_2 observations at a monitoring station and investigates whether it is possible to detect specific fuel signatures in these observations. The Ochsenkopf station introduced in Sect. 4.1 is not used as an example for this comparison for two reasons: The main reason is that the signal at this station is strongly influenced by biospheric activity, thus the observed OR_p is dominated by biospheric activity rather than by fossil fuel use. The second reason (which is true for most other European stations as well) is that the local OR_{ffp} is only slightly higher than the global average and does not exhibit large variations. This combination makes it difficult to detect specific fuel signatures in observations from this station or to assess the performance of the global and regional model against the observations. (An impression of the range of observed oxidative ratios versus the simulated OR_{ff} is given in Fig. 7. The corresponding time series of observed and simulated O_2 and CO_2 measurements and oxidative ratios can be found in Fig. S1 in the Supplement to this paper.)

As an example where observed oxidative ratios are strongly influenced by variations in the local fuel use, we have chosen Hateruma Island, although we cannot show a comparison of the local and the global model at this station as it is not part of the REMO domain. However, this station is particularly interesting for our purpose because of the above mentioned fossil-fuel-related variation in OR_p that has been observed at this station. As explained in Sect. 1, these variations are caused by air masses originating from different Asian countries with different fuel mix signatures.

The Hateruma monitoring station, operated by the National Institute of Enviromental Studies (NIES), Japan, is situated on the eastern edge of Hateruma Island (24°03′ N, 123°48′ E, 10 m a.s.l.). Air is sampled from a small observation tower at a height of 36 m agl. Air masses arriving at Hateruma are mostly influenced by the Asian continent during winter time and from the Pacific Ocean in summer (Tohjima, 2000; Tohjima et al., 2010). As in-situ O_2 measurements started in October 2006, we investigate here the time period from October 2006 to December 2006. For this time period, the fossil fuel contribution to the atmospheric CO_2 signal is expected to be significant: Mostly continental air is measured, and biospheric activities are lower during wintertime.

Figure 6a and b show CO_2 and O_2 observations from Hateruma (represented by brown dots), together with TM3 simulations for CO_{2ff} and O_{2ff} (black lines). Here it can be seen that indeed most of the synoptic variability in the observations is caused by fossil fuel events: Most peaks in CO_2 (and corresponding dips in O_2) correlate with peaks/dips in the fossil fuel simulations. (As already seen in Fig. 5, the peak heights tend to be underestimated by TM3). Figure 6c

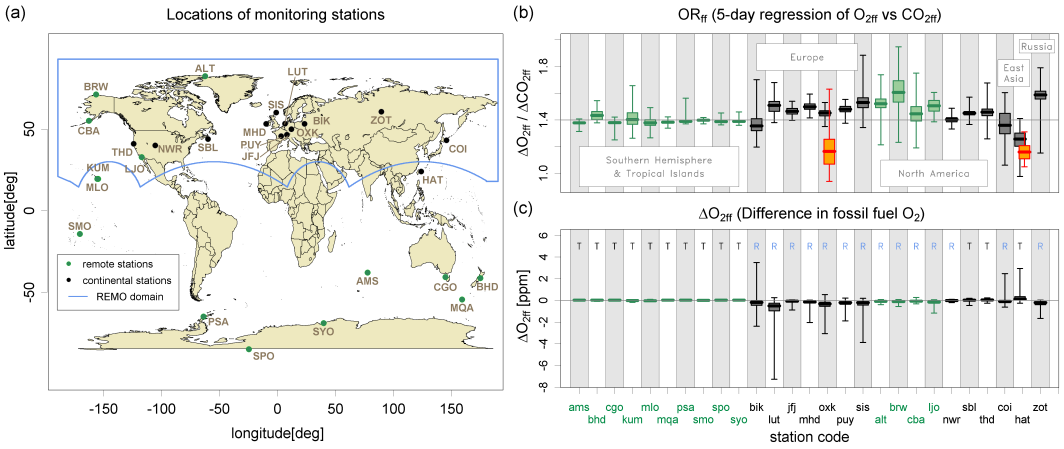

Fig. 7. Perceived fossil-fuel-related oxidative ratio **(b)** and difference in O_2 signal **(c)** from TM3 and REMO model simulations for all available monitoring stations, with their locations shown in **(a)**. The box-and-whisker plots show minimum, maximum, and quartile scores for the year 2006. Labels denote the station code, corresponding to that in the map **(a)**. To facilitate the recognition of continental and remote stations in this plot, labels of remote stations are green, whereas labels of stations on the continent or on islands mainly influenced by continental air masses are black. Simulation output from REMO is used when available, as TM3 tends to underestimate the magnitude of the fossil fuel signals. The letters "R" and "T" indicate whether results from REMO or TM3 are shown for the respective station. For the stations Ochsenkopf (OXK) and Hateruma (HAT), observed oxidative ratios are added to the plot, orange boxes in **(b)**. Note that observations at Hateruma are only performed for the period October to December, while the simulations cover the whole year.

shows the perceived oxidative ratios, determined from the observations (brown) and the simulated values (black), using a 5-day regression as in Fig. 5c. Shaded error bars indicate the respective errors of the linear fit. For oxidative ratios with an error larger than 0.05 (marked in orange), the O_2/CO_2 correlation is considered not to be sufficient for interpretation. The results indicate that a significant part of the observed variability in the oxidative ratios can be captured using the fossil fuel component simulated by even a coarse global model like TM3. This also suggests that the information about the local fuel mix is important for interpreting atmospheric measurements at this station: On the one hand, the assumption of $OR_{ff} = 1.4$ is generally an overestimation here – implementing a constant, but locally correct value (maybe based on the average Asian fuel mix) would already improve the performance of the model. On the other hand, the combination of the observed variability in the oxidative ratio, together with the information on the diverse fuel mix of the surrounding Asian countries can be used for detecting the origin of air masses and thus contributes to the testing and evaluation of transport models. Some more discussion on this issue, together with a detailed analysis of oxidative ratios for different synoptic events is found in (Minejima et al., 2011)

4.3 Potential effects of variable OR_{ff} at other monitoring stations

With Hateruma Island we have presented an example where the effects of variable oxidative ratios need to be taken into account when interpreting atmospheric oxygen measurements. The question is whether these effects also play a significant role for other stations in the global monitoring network. Figure 7 illustrates results from REMO and TM3 simulations for all oxygen monitoring stations where output from one or both of the models exist. Figure 7a gives an overview of the station locations, also indicating the range of the REMO domain. The box-and-whisker-plot in Fig. 7b gives the distribution of OR_{ffp} for the year 2006, determined from the 5-day running regression of O_{2ff} versus CO_{2ff}, for the aforementioned stations Ochsenkopf and Hateruma Island we have included the distribution for the observed oxidative ratios as well (shown in orange). Figure 7c shows the difference ΔO_{2ff} caused by the variable OR_{ff} as defined in Sect. 4.1. Since both models show similar results for oxidative ratios on the synoptic timescale investigated here (see Fig. 5), both of them can be used for the respective set of stations, depending on their availability. For the difference ΔO_{2ff} results from the regional model are used where available, since they presumably capture the fossil-fuel-related variations better. As this needs to be taken into account when comparing the magnitude of signals at different stations, the letter "R" or "T" next to each station's results indicates whether output from REMO or TM3 is used.

Stations located on the Southern Hemisphere and on tropical islands usually receive a well-mixed background fossil-fuel signal instead of being influenced by local sources. Hence, their perceived oxidative ratio shows only small variations and its median does not differ significantly from the global average. For European, Asian and North American stations, variations in OR_{ffp} are larger. Besides, deviations

of their median OR_{ffp} from the global average are in accordance with the results for the O_2/CO_2 emission ratios in Fig. 2c: the median is slightly higher for Europe and North America, significantly higher for the Russian station (Zotino Tall Tower Observatory (ZOT), located in Siberia) and lower for the two Eastern Asian Stations (one of them being Hateruma (HAT)). As expected, variations in OR_{ff} and deviations from the global average are generally larger for continental stations or stations with dominant continental influence (recognizable by the black symbols) than for remote stations (marked by green symbols). Nevertheless also some of the remote stations, e.g. Alert (ALT, Canada) or Barrow (BRW, Alaska), exhibit larger variations in OR_{ffp}. However, as seen from Fig. 7b, large variations in the oxidative ratios do not necessarily lead to detectable changes in the atmospheric signal at the station. If the fossil-fuel-related CO_2 and O_2 signals are small, as it is the case for the remote stations, variations in OR_{ffp} do not cause any significant difference $\Delta O2_{ff}$. In contrast, differences range between -8 and +4 ppm for continental stations, being largest for stations located in the vicinity of fossil fuel sources with a non-standard fuel mix, e.g. Hateruma in Asia or Lutjewad in the Netherlands.

The use of a global average OR_{ff} of 1.4 can therefore be regarded as sufficient when only interpreting data from remote stations. For continental stations, however, the influence of local fuel sources, especially those with a non-standard fuel mix, can lead to detectable changes in the atmospheric O_2 signals. For the stations where model output from TM3 is used, the fossil-fuel-related atmospheric signals are presumably larger than in the simulations as the global model tends to underestimate the magnitude of the synoptic scale signals. In addition, variations in fossil fuel emissions occurring on scales smaller than the $1^\circ \times 1^\circ$ resolution of the COFFEE dataset (e.g. emissions from point sources as power plants) are not taken into account, but might have an additional impact on the synoptic scale OR_{ffp}.

Whether the contribution of OR_{ffp} to the total atmospheric oxidative ratio is significant, depends on the relative strengths of fossil fuel signals compared to the influence of other processes, e.g. related to biospheric activity. The signal at Ochsenkopf station, for example, is strongly influenced by biospheric signals, as already mentioned in Sect. 4.2. This can also be seen in Fig. 7b – the observed oxidative ratios are mostly much lower than the simulated OR_{ffp}. Hence the possibility to use fossil-fuel-related oxidative ratios for identification of emission sources or improvement of atmospheric transport is also subject to the strengths of these other sources and sinks at a given station.

5 Impact of variable oxidative ratios on APO fluxes

Spatial and temporal variations in fuel use are also likely to influence the calculation of oceanic and biospheric fluxes derived from atmospheric O_2 and CO_2 measurements. To isolate the oceanic component from measured oxygen signals, usually the tracer APO = ΔO_2+ 1.1 ΔCO_2 (Stephens et al., 1998) is used. Whereas APO is by definition not changed by biospheric processes (at least to the extent where OR_{bio} agrees with the global average of $\alpha_B = 1.1$), the influence from fossil fuel burning is reduced, but still present in the signal. This is usually accounted for by using fossil fuel statistics to calculate a fuel-corrected APO signal (assuming a constant value for OR_{ff}). A well-established method to interpret measured APO signals in terms of surface fluxes is the atmospheric transport inversion (Enting et al., 1995), applied to APO by Rödenbeck et al. (2008). For this method, spatial and temporal variations in the atmospheric tracer concentration at measurement locations are simulated using a transport model. By minimizing the differences between observed and model-derived concentrations, the contributing surface fluxes are estimated using inverse techniques.

Here we investigate whether it is necessary to include variable OR_{ff} in APO inversions to avoid mistaking fossil-fuel-related variations for signals caused by ocean processes. For this, we performed an APO inversion following that of Rödenbeck et al. (2008). We used the "standard setup" described in that paper (Sect. 2.4) with TM3 as a transport model. As observational input, atmospheric CO_2 and O_2 data from 16 measurement sites (in the following referred to as 'inversion stations') were used. These data result from the measurement programs of the Scripps Institute of Oceanography (Manning and Keeling, 2006; Keeling and Shertz, 1992), the Princeton University (Bender et al., 1996; Battle et al., 2006) and the Japanese National Institute for Environmental Studies (Tohjima et al., 2003). Sampling at these stations started at different times between 1991 and 1999. To avoid spurious flux variations in the inversion calculations caused by the sudden appearance of a new station in the observational dataset, we only used the time period from 1999 to 2005 where records from all 16 sites contain reliable data. Fluxes were calculated from the year 1996 on to allow for sufficient spin-up time of the model, but only results from 1999 on are considered for further analysis. For testing the effects of variable oxidative ratios, a synthetic dataset was created, containing the simulated difference $\Delta APO_{ff} = APO_{ff}$ ($OR_{ff} = OR_{COFFEE}$) – APO_{ff} ($OR_{ff} = 1.4$) at the monitoring stations. These APO differences were inverted, resulting in a set of flux differences $\Delta F_{APO\,ff}$. Since the inversion can only adjust the ocean fluxes, differences caused by non-constant oxidative ratios are attributed to ocean fluxes. To quantify the fossil fuel effects on different timescales, we applied two sets of filters to the results: in Sect. 5.1, we are focusing on long-term biases and interannual variability, in Sect. 5.2 we investigate effects on the seasonal cycle.

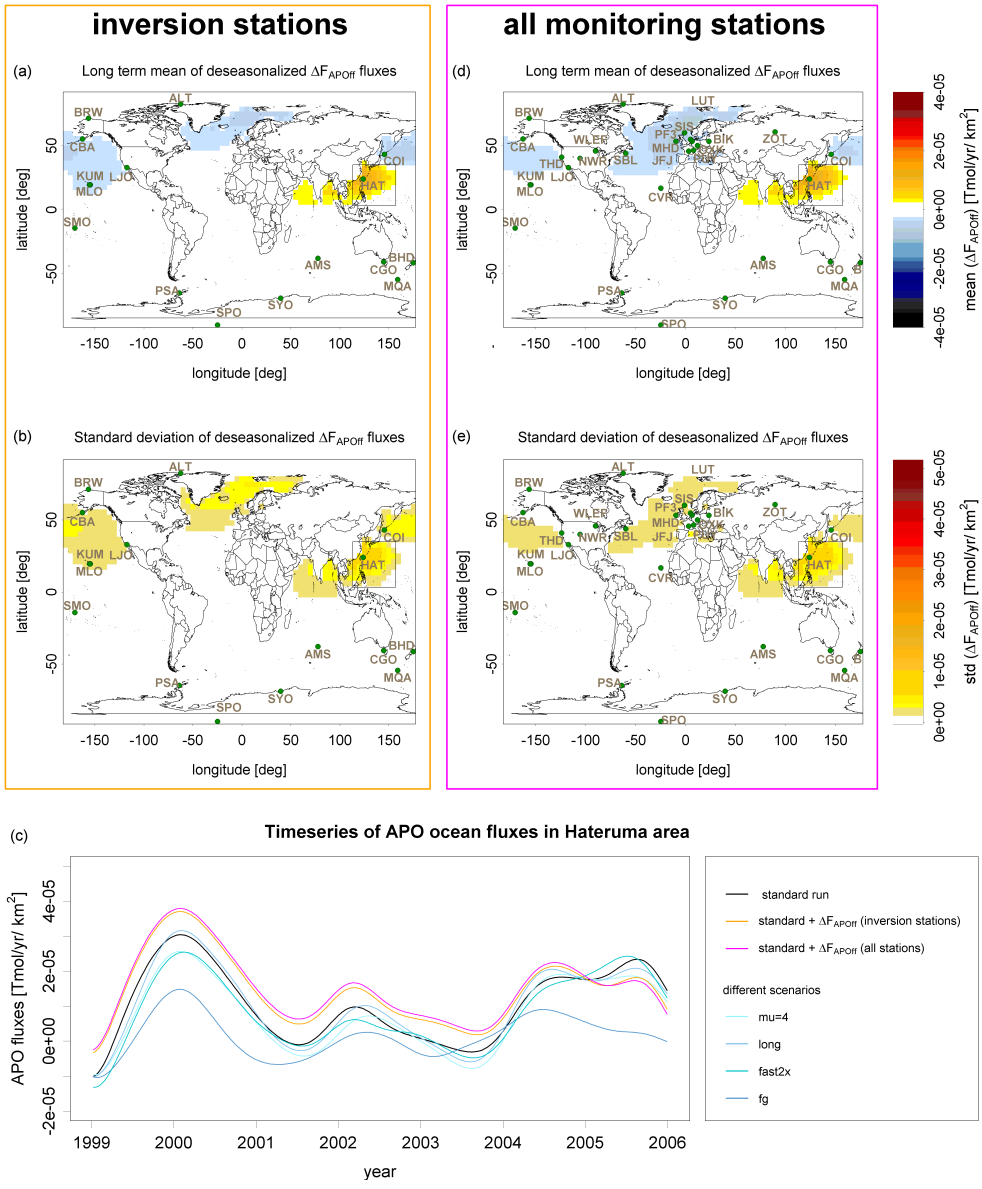

Fig. 8. Influence of variable oxidative ratios on APO fluxes on multi-year and interannual timescales, derived from global APO inversion. Shown are the fossil-fuel-related fluxes $\Delta F_{APO_{ff}}$ that are mistaken for ocean signals when ignoring variation in OR_{ff}. The upper row **(a, d)** shows the long-term mean of $\Delta F_{APO_{ff}}$ as indicator for systematic biases, the middle row **(b, e)** the deseasonalized temporal standard deviation as measure for temporal variability. The left column shows inversion results using the station set from Rödenbeck et al. (2008), the right column the results using all monitoring stations currently measuring atmospheric O_2 and CO_2. For the area around Hateruma (black box), $\Delta F_{APO_{ff}}$ for both scenarios is compared to the size of the real ocean fluxes F_{APO} (black) and their uncertainty (blue).

5.1 Long-term mean and interannual variability

For characterizing the influence of variable oxidative ratios on APO fluxes on multi-year and interannual timescales, the mean seasonal cycle and most variations faster than one year were subtracted from the results (using the filter "Filt0.5gd", described by Rödenbeck, 2005). Figure 8 shows global maps of the filtered $\Delta F_{APO_{ff}}$ fluxes, with Figure 8a depicting the long-term mean of $\Delta F_{APO_{ff}}$ (indicating systematic offsets in the APO fluxes) and Fig. 8b the temporal standard deviation of the filtered fluxes as a measure for the interannual variability. A dominant feature in both plots is seen around the Hateruma monitoring station, consistent with the results from Sects. 4.2 and 4.3. Since the fossil-fuel-related oxidative ratio influencing the atmospheric signal at this station is significantly lower than the global average, the assumption of $OR_{ff} = 1.4$ leads to an overestimation of the oceanic APO fluxes in that region (and thus a positive $\Delta F_{APO_{ff}}$ offset in

the long-term mean, see Fig. 8a). The same effect also causes an increase in the interannual variability in the Hateruma region (Fig. 8b). In addition, most of the other features in Fig. 8a and b, e.g. the negative offset and higher variability in the Northern Pacific, can be attributed to far-field effects of the overestimation of OR_{ff} at Hateruma. This was tested by running another inversion without the Hateruma station.

To assess the significance of these effects, we compare the resulting differences to the magnitude of the APO ocean fluxes F_{APO} (as determined from the standard inversion) and their uncertainties. Figure 8c shows time series of F_{APO} calculated with constant (black) and variable (orange) OR_{ff} for the Hateruma region (i.e. the area enclosed by the box in Fig. 8 a and b). For characterizing the uncertainties of F_{APO}, we compare the "standard run" to an ensemble of runs where specific setup details were varied. To cover the range of uncertainties realistically, we have varied the inversion parameters to which the resulting fluxes are most sensitive (according to Rödenbeck et al., 2008): tightness of the a priori constraint relative to the data constraint ("$\mu = 4$"), scales of the spatial and temporal smoothing ("long" – increased a priori correlation length, "fast2x"- decreased a priori correlation time) and resolution of the transport model ("fg" – fine grid ($4^\circ \times 5^\circ \times 19$ vertical levels) instead of coarse grid ($\approx 8^\circ \times 10^\circ \times 9$ vertical levels)). The fluxes F_{APO} resulting from these different scenarios are shown in different shades of blue in Fig. 8c. The plot reveals that the fossil-fuel-related differences $\Delta F_{APO_{ff}}$ in the Hateruma area are comparable to the uncertainty given by the ensemble range. It is therefore recommended to include the information on variable OR_{ff} when using data from such a station. When removing the Hateruma station from the stationset for the inversion, the resulting $\Delta F_{APO_{ff}}$ become negligible. This is due to the fact that apart from the second Japanese station Cape Ochi-Ishi (COI), the remaining "inversion stations" are typical remote stations, most of them located on the Southern Hemisphere. As already seen in Sect. 4.3, the influence of local fuel sources is insignificant at these locations.

Continental – and therefore likely more polluted – monitoring stations are currently not included in the set of stations used for the inversion. Since atmospheric measurements at an increasing number of continental stations have become available in the recent decade, future inversions will probably include data from this kind of stations. It is thus worth investigating whether fossil-fuel-related effects from these stations can be as significant as the effects caused by the Hateruma station. Therefore a further synthetic experiment was performed, using a new set of pseudo-data for all monitoring stations that currently measure O_2/N_2 and CO_2. To avoid artifacts due to different sampling frequencies or differences in the start of the measurements, weekly sampling at every station was assumed over the whole time period. The resulting $\Delta F_{APO_{ff}}$ fluxes are shown in Fig. 8 d and e. In analogy to the results for the inversion stations, Figure 8d shows the long-term mean and Fig. 8e the standard deviation of $\Delta F_{APO_{ff}}$. Station locations are included in both maps. It can be seen that the addition of continental stations does not change the global picture completely. As most of the additional stations are located in Europe or North America, main differences occur in the Northern Atlantic, the Mediterranean Sea and the North Sea. Here the negative offset in the long-term mean becomes stronger, reaching up to $\sim$50 % of the F_{APO} signals in this region. This negative bias is in accordance with OR_{ff} being slightly higher than 1.4 for Europe and North America and thus becoming underestimated in the standard inversion. This also causes a higher interannual variability of $\Delta F_{APO_{ff}}$ in the mentioned regions.

On the other hand, both the negative offset and the amplitude of the interannual variability are reduced in the Pacific Area; the interannual variability is also lower in the Arctic Ocean. From the inversion with the smaller stationset, $\Delta F_{APO_{ff}}$ fluxes in these areas were already identified as far-field effects from the Hateruma station. With the inclusion of the additional European and North American stations, fluxes in the North Atlantic and North Pacific are now better constrained. Therefore, the inversion algorithm has less freedom to distribute the excess fluxes globally. These fluxes are now more localized in the Hateruma region; in this area both offset and interannual variability are slightly higher in the inversion setup with the continental stations.

5.2 Seasonality

To investigate the effect of seasonal variations in fuel use on the seasonal cycles of F_{APO}, we extracted the mean seasonal cycle from the inversion results (using the triangular filter 'Filt6.0Tm' from Rödenbeck (2005)). As only annual averages for fossil fuel CO_2 emissions are used in global APO inversions, the seasonal component of $\Delta F_{APO_{ff}}$ can be influenced by seasonal variations in both CO_{2ff} and OR_{ff}, i.e. by variations in the amount and the type of fuel used, respectively. To separate these two effects, we performed an additional inversion of APO pseudodata containing the CO_2 seasonality as in COFFEE, but only using $OR_{ff} = 1.4$.

The range of the resulting seasonal variations is shown in Fig. 9, with Figure 9a showing the influence of seasonal variations in the CO_2 emissions and Fig. 9b the effects due to variations in the oxidative ratios. Differences in the seasonal cycle occur mainly in the Northern Hemisphere, being highest in the North Atlantic and in the area around Hateruma. In general, the effect of variability in OR_{ff} is stronger than that of the seasonality in CO_2 emissions. However, the seasonal $\Delta F_{APO_{ff}}$ fluxes are small against the seasonal amplitudes of F_{APO} and their uncertainties. This is seen in Fig. 9c, illustrated by a time series for the region with the highest $\Delta F_{APO_{ff}}$ fluxes (indicated by the black box in Fig. 9a and b). In analogy to Figure 8c, the black line shows the seasonal F_{APO} fluxes and the blue lines the ensemble of runs characterizing their uncertainty. The results represented by the orange line take into account the total $\Delta F_{APO_{ff}}$, i.e.

the sum of the effects caused by CO_2 seasonality and variable OR_{ff}. Here only the results from the 'inversion stations' are shown, as the results from the "all monitoring stations" runs do not show any significant differences to the runs with the "inversion stations".

6 Conclusions

We have presented a global dataset of CO_2 emissions and O_2 uptake associated with fossil fuel burning, created from emission inventories and fuel consumption data. We have used this dataset to characterize the range of spatial and temporal variations of oxidative ratios OR_{ff} from fossil fuel combustion, and to investigate the influence of these variations on atmospheric oxygen signals. The "CO_2 release and Oxygen uptake from Fossil Fuel Emission Estimate" (COFFEE) dataset contains hourly resolved anthropogenic CO_2 emissions and the corresponding O_2 uptake for the years 1996 to 2008 on a $1° \times 1°$ grid. It is available for download at ftp://ftp.bgc-jena.mpg.de/pub/outgoing/coffee.

Spatial variations in the O_2/CO_2 emission ratios resulting from COFFEE show clear differences in the fuel mix of different regions, with OR_{ff} covering the whole range from 0 to 1.95 and having a spatial standard deviation of 0.2. Temporal variations in OR_{ff} occur on different timescales: Long-term changes show differences ranging from -0.2 to 0.3 per decade on gridcell level, with no predominant trend in either direction. In addition, OR_{ff} is varying due to seasonal and short-term variations in fuel use, with variations on daily level dominating, especially in the Southern Hemisphere and the Tropics. In general, however, the range of temporal variations is rather small compared to that of the spatial differences, especially taking into account that the temporal factors included in our dataset tend to overestimate the sub-annual variability.

Spatially averaged across the whole globe, the mean OR_{ff} calculated from COFFEE varies between 1.39 and 1.42 from year to year, and thus does not differ significantly from the commonly used value of $\alpha_F = 1.4$. The α_F derived from the COFFEE dataset shows a downward trend starting from the year 2000 on, related to increasing CO_2 emissions from coal burning. This shift in fuel use is attributed to a growing contribution of CO_2 emissions from China and other countries where coal is the main fuel source. Despite this recent trend, temporal variations in α_F are too small to have significant influence on the partitioning of global carbon sinks.

The influence of variable OR_{ff} on the atmospheric oxygen signals at ground-based monitoring stations was investigated using model simulations from the TM3 and REMO models with the COFFEE dataset as input. Fossil-fuel-related O_2 and CO_2 signals at the stations are mainly influenced by synoptic scale events. Expectedly, the perceived OR_{ff} on synoptic time scales shows larger variations and deviations of its mean from the global average for continental monitoring stations than for the classical remote stations. Depending on the magnitude of fossil-fuel-related CO_2 fluxes at the measurement location, the influence of the local fuel mix can change the atmospheric O_2 mixing ratio by several ppm. Whether these effects can be detected in atmospheric CO_2 and O_2 observations has been examined for the case of the Hateruma monitoring station. As this station

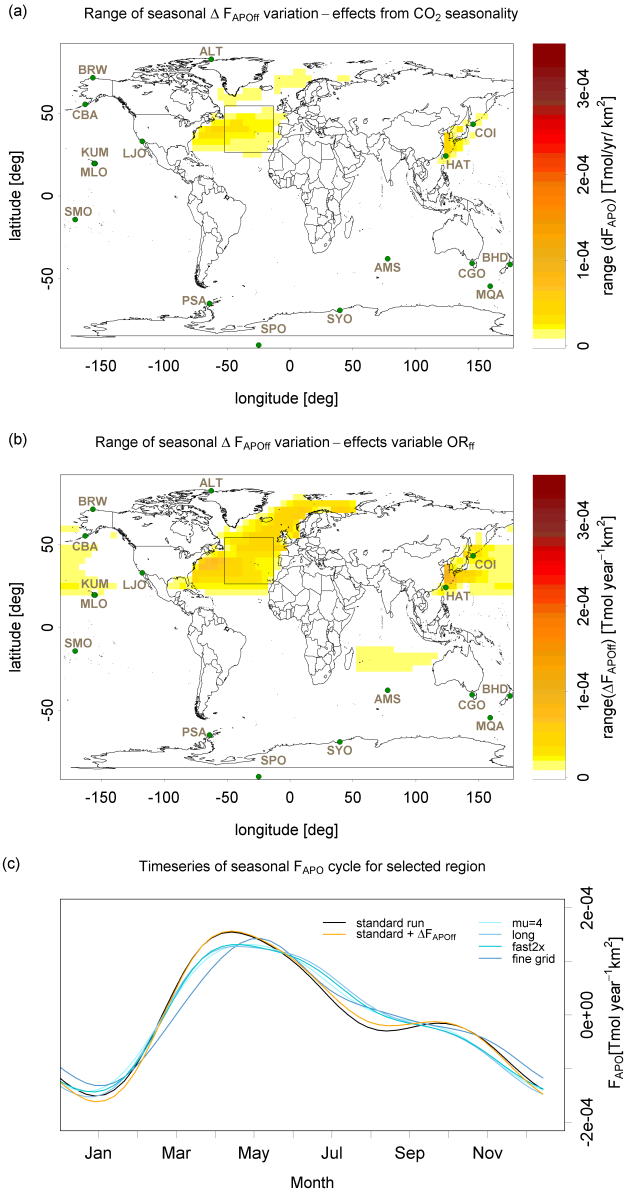

Fig. 9. Influence of variable oxidative ratios on APO fluxes on seasonal timescales. The maps show the amplitude of the seasonal component of the $\Delta F_{APOff,}$ split into the part that is caused by seasonal variations in CO_2 **(a)** and the part that is caused by variations in OR_{ff} **(b)**. For the area with the largest $\Delta F_{APO}{}_{ff}$ fluxes (indicated by the black box), the total resulting flux $\Delta F_{APO}{}_{ff}$ is compared to the size of the real ocean fluxes F_{APO} (black) and their uncertainty (blue).

often receives polluted air from several Asian countries with differing OR_{ff}, the information on the local fuel mix is crucial for interpreting observations there and can potentially be used for identifying the origin of airmasses. Whether this information is required to interpret data for other stations as well or can even be used to identify specific emission sources, depends on the individual station and investigated time period (e.g. summer/winter), as the size of the fossil fuel signal in comparison to signals from other processes (e.g. biospheric) plays a role as well. For these investigations, the use of regional models with a higher resolution is recommended, as the global model used here tends to underestimate the magnitude of synoptic events that dominate the variation in OR_{ff}. In the case of remote monitoring stations, however, fossil fuel signals and thus the influences of variable OR_{ff} are mostly negligible. In addition, most of the existing continental stations that are influenced by local fossil fuel sources are located in Europe or North America, where the average OR_{ff} does not differ much from 1.4. An exception is the station Lutjewad in the Netherlands, where the high usage of natural gas makes it necessary to use a higher OR_{ff}. Here the COFFEE dataset has already been used successfully for the separation of the fossil fuel part from APO signals (van der Laan-Luijkx et al., 2010).

Variations in OR_{ff} might also play a significant role for other European and North American stations, when airmasses are influenced by local fuel sources that deviate from the average mix of the country (e.g. power plants, cement production). However, it remains to be investigated whether the $1^\circ \times 1^\circ$ resolution of the COFFEE dataset is sufficient to account for this. Currently, we are in the progress of updating the dataset to a higher resolved version, based on the $0.1^\circ \times 0.1^\circ$ fossil fuel emissions from EDGAR 4.1. (Once finished, the new version will be available for download at the same website, information on the updating process and detailed description can be found at www.bgc-jena.mpg.de/bgc-systems → Download → COFFEE). In addition, the oxidative ratios on the usage type/country level could also be easily combined with other fossil fuel inventories, for example the Vulcan inventory for the US (Gurney et al., 2009) or the IER inventory (Institut für Energiewirtschaft und Rationelle Energieanwendung, University of Stuttgart, http://carboeurope.ier.uni-stuttgart.de/) for Europe. For potential future monitoring stations in regions such as South America, Africa or Asia, at least the information on the average local OR_{ff} and thus the spatial component of COFFEE is useful.

As one of the main applications of atmospheric oxygen measurements is the calculation of oceanic carbon sinks, we have investigated the possibility that variations in OR_{ff} could be mistaken for oceanic signals. For that we calculated long-term, interannual and seasonal oceanic fluxes for constant and variable OR_{ff}, using a global APO inversion. Whereas the resulting differences in the seasonal cycle are in general negligible, long-term biases and differences in the interannual variability can be significant. This is strongly depending on the stationset chosen for the observational input: When using only remote stations, fossil fuel effects are expectedly negligible, but as soon as data from the Hateruma monitoring station is included, the local overestimation of OR_{ff} leads to – both local and far-field – differences in the fluxes. The addition of data from existing non-remote monitoring stations in North America and Europe to the inversion partly counteracts the effects caused by the overestimation of OR_{ff} at Hateruma, but also causes an additional bias in the North Atlantic due to the slight underestimation of the OR_{ff} in European and North America. The resulting effects can be as large as the uncertainties of the inversion. Thus, we recommend taking into account the spatially variable oxidative ratios such as those provided by the COFFEE dataset. For regional inversions, the influence is likely to be larger, making variable oxidative ratios more important.

Altogether the COFFEE dataset has proven to be a useful tool for quantifying the effects of variable oxidative ratios from fuel combustion. We have shown that while for interpretation of observations from remote stations and many global implementations the use of a constant global average is sufficient, there are applications where more precise information on fossil-fuel-related oxidative ratios is needed.

Supplement related to this article is available online at: http://www.atmos-chem-phys.net/11/6855/2011/acp-11-6855-2011-supplement.pdf.

Acknowledgements. This work has been partially funded through the 7th framework EU project ICOS (contract No. 211574). We thank Yasunori Tohjima and Hiroaki Yamagishi (ResearcherID B-3174-2009) for performing in-situ oxygen measurements at Hateruma Island, and Rona Thompson and the MPI-BGC tall tower group for in-situ measurements at Ochsenkopf. We are also grateful to Ralph Keeling, Andrew Manning, Yasunori Tohjima, Michael Bender and Nicolas Cassar for providing their CO_2 and O_2 data for use in the APO inversion, and all their coworkers who had contributed to obtaining these data.

The service charges for this open access publication have been covered by the Max Planck Society.

Edited by: R. Harley

References

Battle, M., Bender, M. L., Tans, P. P., White, J. W. C., Ellis, J. T., Conway, T., and Francey, R. J.: Global carbon sinks and their variability inferred from atmospheric O_2 and $\delta^{13}C$, Science, 287, 2467–2470, 2000.

Battle, M., Mikaloff Fletcher, S. E., Bender, M. L., Keeling, R. F., Manning, A. C., Gruber, N., Tans, P. P., Hendricks, M. B., Ho, D. T., Simonds, C., Mika, R., and Paplawsky, B.: Atmospheric potential oxygen: New observations and their implications for

some atmospheric and oceanic models, Global Biogeochem. Cy., 20, GB1010, doi:1010.1029/2005GB002534, 2006.

Bender, M., Ellis, T., Tans, P., Francey, R., and Lowe, D.: Variability in the O_2/N_2 ratio of southern hemisphere air, 1991–1994: Implications for the carbon cycle, Global Biogeochem. Cy., 10, 9–21, 1996.

Bender, M., Battle, M., and Keeling, R. F.: The O_2 Balance of the Atmosphere: A Tool for Studying the Fate of Fossil-Fuel CO_2, Ann. Rev. Ener. Environ., 23, 207–223, 1998.

Boden, T. A., Marland, G., and Andres, R. J.: Global, Regional, and National Fossil-Fuel CO_2 Emissions from Fossil-Fuel Burning, Cement Manufacture, and Gas Flaring: 1751–2006 Carbon Dioxide Information Analysis Center, Oak Ridge National Laboratory, US Department of Energy, Oak Ridge, Tenn., USA, doi:10.3334/CDIAC/00001, 2009.

BP (British Petroleum): Statistical Review of World Energy: http://www.bp.com/statisticalreview, last access: December 2010, 2009.

Brenkert, A. L.: Carbon Dioxide Emission Estimates from Fossil-Fuel Burning, Hydraulic Cement Production, and Gas Flaring for 1995 on a One Degree Grid Cell Basis, Carbon Dioxide Analysis Center, Oak Ridge, Tenn., USA, 1996.

Chevillard, A., Karstens, U., Ciais, P., Lafont, S., and Heimann, M.: Simulation of atmospheric CO_2 over Europe and western Siberia using the regional scale model REMO, Tellus Ser. B-Chem. Phys. Meteorol., 54, 872–894, 2002.

EDGAR/PBL: Temporal variation of anthropogenic sources, http://themasites.pbl.nl/en/themasites/edgar/documentation/content/Temporal-variation.html, European Commission, Joint Research Centre (JRC)/Netherlands Environmental Assessment Agency (PBL), last access: May 2011, 2010.

Enting, I. G., Trudinger, C. M., and Francey, R. J.: A synthesis inversion of the concentration and $\delta^{13}C$ of atmospheric CO_2, Tellus B – Chem. Phys. Meteorol., 47, 35–52, 1995.

Francey, R. J., Trudinger, C. M., Schoot, M. V. d., Krummel, P. B., Steele, L. P., and Langenfelds, R. L.: Differences between trends in atmospheric CO_2 and the reported trends in anthropogenic CO_2 emissions, Tellus B – Chem. Phys. Meteorol., 62, 316–328, doi:10.1111/j.1600-0889.2010.00472.x, 2010.

Gurney, K. R., Mendoza, D., Zhou, Y., Fischer, M., de la Rue du Can, S., Geethakumar, S., and Miller, C.: The Vulcan Project: High resolution fossil fuel combustion CO_2 emissions fluxes for the United States, Environ. Sci. Technol., 43, 5535–5541, doi:10.1021/es900806c, 2009.

Heimann, M. and Körner, S.: The global atmospheric tracer model TM3.Technical Report 5, Max Planck Institute for Biogeochemistry, Jena, Germany, 2003.

IEA: CO_2 emissions from fossil fuel combustion: 1971–2005 (2007 edition), International Energy Agency, 2007.

Keeling, R. F.: Development of an interferometric analyzer for precise measurements of the atmospheric oxygen mole fraction, PhD thesis, Harvard University, Cambridge, Massachusetts, USA, 178 pp., 1988.

Keeling, R. F. and Shertz, S. R.: Seasonal and interannual variations in atmospheric oxygen and implications for the global carbon cycle, Nature, 358, 723–727, 1992.

Keeling, R. F., Najjar, R. P., Bender, M. L., and Tans, P. P.: What atmospheric oxygen measurements can tell us about the global carbon cycle?, Global Biogeochem. Cy., 7, 37–67, 1993.

Langmann, B.: Numerical modelling of regional scale transport and photochemistry directly together with meteorological processes, Atmos. Environ., 34, 3585–3598, 2000.

Manning, A. C. and Keeling, R. F.: Global oceanic and land biotic carbon sinks from the Scripps atmospheric oxygen flask sampling network, Tellus B – Chem. Phys. Meteorol., 58, 95–116, 2006.

Minejima, C., Kubo, M., Tohjima, Y., Yamagishi, H., Koyama, Y., Maksyutov, S., Kita, K., and Mukai, H.: Analysis of $\Delta O_2/\Delta CO_2$ ratios for the pollution events observed at Hateruma Island, Japan, Atmos. Chem. Phys. Discuss., 11, 15631–15657, doi:10.5194/acpd-11-15631-2011, 2011.

Olivier, J. G., and Berdowski, J. J. M.: Global emission sources and sinks., in: The Climate System: 33–77, edited by: Berdowski, J., Guicherit, R., and Heij, B. J., Lisse: Swets & Zeitlinger Publishers, 2001.

Rödenbeck, C.: Estimating CO_2 sources and sinks from atmospheric mixing ratio measurements using a global inversion of atmospheric transport. Technical Report 6, Max Planck Institute for Biogeochemistry, Jena, Germany, 2005.

Rödenbeck, C., Le Quere, C., Heimann, M., and Keeling, R. F.: Interannual variability in oceanic biogeochemical processes inferred by inversion of atmospheric O-2/N-2 and CO_2 data, Tellus B – Chem. Phys. Meteorol., 60, 685–705, 2008.

Severinghaus, J. P.: Studies of terrestrial O2 and Carbon Cycles in Sand Dune Gases an in Biosphere 2., PhD thesis, Columbia University, New York, USA, 148 pp., 1995.

Sirignano, C., Neubert, R. E. M., Meijer, H. A. J., and Rödenbeck, C.: Atmospheric oxygen and carbon dioxide observations from two European coastal stations 2000–2005: continental influence, trend changes and APO climatology, Atmos. Chem. Phys. , 10, 1599–1615, doi:10.5194/acp-10-1599-2010, 2010.

Stephens, B. B., Keeling, R. F., Heimann, M., Six, K. D., Murnane, R., and Caldeira, K.: Testing global ocean carbon cycle models using measurements of atmospheric O_2 and CO_2 concentration, Global Biogeochem. Cy., 12, 213–230, 1998.

Thompson, R. L., Manning, A. C., Gloor, M., Schultz, U., Seifert, T., Haensel, F., Jordan, A., and Heimann, M.: In-situ measurements of oxygen, carbon monoxide and greenhouse gases from Ochsenkopf tall tower in Germany, Atmos. Meas. Tech., 2, 573–591, doi:10.5194/amt-2-573-2009, 2009.

Tohjima, Y.: Method for measuring changes in the atmospheric O-2/N-2 ratio by a gas chromatograph equipped with a thermal conductivity detector, J. Geophys. Res.-Atmos., 105, 14575–14584, 2000.

Tohjima, Y., Mukai, H., Machida, T., and Nojiri, Y.: Gas-chromatographic measurements of the atmospheric oxygen/nitrogen ratio at Hateruma Island and Cape Ochi-ishi, Japan, Geophys. Res. Lett., 30, 1653, doi:1610.1029/2003GL017282, 2003.

Tohjima, Y., Mukai, H., Hashimoto, S., and Patra, P. K.: Increasing synoptic scale variability in atmospheric CO_2 at Hateruma Island associated with increasing East-Asian emissions, Atmos. Chem. Phys., 10, 453–462, doi:10.5194/acp-10-453-2010, 2010.

United Nations Statistics Division: Energy Statistics Database: http://data.un.org/, last access: December 2010, 2009.

van der Laan-Luijkx, I. T., Karstens, U., Steinbach, J., Gerbig, C., Sirignano, C., Neubert, R. E. M., van der Laan, S., and Meijer, H. A. J.: CO_2, δO2/N2 and APO: observations from the

Lutjewad, Mace Head and F3 platform flask sampling network, Atmos. Chem. Phys., 10, 10691–10704, doi:10.5194/acp-10-10691-2010, 2010.